SYNTHETIC SEISMIC REFLECTION MODELLING IN THE SUPERCRITICAL GEOTHERMAL SYSTEM OF THE LARDERELLO FIELD (ITALY)

R. de Franco[1], L. Petracchini[2], D. Scrocca[2], G. Caielli[1], G. Montegrossi[3], A. Santilano[4], A. Manzella[4]

[1] Istituto per la Dinamica dei Processi Ambientali, CNR, Milano, Italy

[2] Istituto di Geologia Ambientale e Geoingegneria, CNR, Roma, Italy

[3] Istituto di Geoscienze e Georisorse, CNR, Pisa, Italy

[4] Istituto di Geoscienze e Georisorse, CNR, Firenze, Italy

Keywords: Larderello, supercritical geothermal system, K-horizon, synthetic seismic profile

ABSTRACT

Synthetic seismic reflection modelling is a useful tool for geothermal exploration as it represents a remarkable support to calibrate geological-geophysical interpretations and model reconstructions, and to explore future seismic reflection acquisition and processing scenarios in geothermal prospecting.

The aim of this work is to test the synthetic seismic reflection modelling along a seismic line (CROP-18A) crossing the historical site of Larderello geothermal field which, with its numerous wells and data, represents a valuable site to calibrate advanced exploration techniques in a potential supercritical geothermal system. The CROP-18A, as many others in the study area, is characterized by a discontinuous but locally very bright seismic marker, named K-horizon, which has been associated to various geological processes, among which to the presence of fluids at supercritical condition. The main effort of this work is oriented to test and verify the potentiality of synthetic seismic reflection modelling to the comprehension of the nature of the K-horizon. Two geophysical models are used to test the seismic response of the K-horizon, which is associated to 1) a lithological discontinuity, or 2) a “Physically Perturbed Layer”, represented by a randomized velocity distribution in a thin layer.

Despite the reliable calibration implied by the use of a lithological discontinuity, the seismic modelling clearly shows that the “Physical Perturbed Layer” explains better the reflectivity features associated to the K-horizon.

1. INTRODUCTION

Synthetic seismic reflection modelling allows to determine prospective features on acquired seismic reflection data and to calibrate the geological-geophysical interpretation and model reconstructions (Riedel et al, 2015; Schmelzbach et al., 2016; Rabbel et al., 2017 and references therein).

In this work, we present the results of a study made in the Lago Boracifero sector of the Larderello geothermal field (Italy). In the Larderello field, superheated steam is at the present exploited from a shallow and a deep reservoir, the latter located in crystalline rocks (Minissale, 1991; Barelli et al., 1995; Bertani et al., 2005; Bertini et al., 2006; Romagnoli et al., 2010; Gola et al., 2017 and references therein).

2D and 3D seismic surveys of the Larderello geothermal field show the presence of a deep seismic marker, named K-horizon (Batini et al., 1978). The K-horizon is characterized by a band of diffused reflectivity associated with lateral variations in reflectivity and occasionally by a bright spot appearance (Batini et al., 1978; Cameli et al., 1993; Ciuffi and Casini, 2018). Several processes have been proposed to interpret the origin of the K-horizon (Cameli et al., 1993; Marini and Manzella, 2005; Brogi et al., 2003; Bertini et al., 2006; Finetti et al., 2001; Vanorio et al., 2004; De Matteis et al, 2008; Liotta and Ranalli, 1999; Tinivella et al., 2005).

The San Pompeo 2 well reached the vicinity of the K-horizon. Temperature > 400° and pressure > 24 MPa have been extrapolated to the depth of 2930 m, (Batini et al., 1983). Following these results, the presence of supercritical fluids confined in a relatively thin layer has also been proposed to explain the high reflectivity of the K-horizon (Bertini et al., 2006).

Our study had four main aims: 1) the calibration of a 2D seismic lines CROP-18A, acquired in the Italian deep crust seismic project (Scrocca et al., 2003); 2) the definition of a conceptual model of the area based on a rock physics model; 3) the modelling of the seismic response of the 3D geological-geophysical model with associated implications for processing the seismic reflection data; 4) the definition of the seismic signature of reservoir rocks possibly hosting supercritical fluids. This proceedings is a synthetic version of the paper

"Synthetic seismic reflection modelling in a supercritical geothermal system: an image of the K-horizon in the Larderello field (Italy)" by de Franco et al. (2019) accepted on the Geofluids special issue titled "Geothermal Systems: Interdisciplinary Approaches for an Effective Exploration".

2. STRATIGRAPHY

The stratigraphic scheme (Figures 1 and 2) adopted in this work (Bertini et al., 2006 and references therein) is made up, from top to bottom by: i. Neoautoctonous complex made of marine, lacustrine and continental deposits (Miocene - Quaternary); ii. Ligurian complex made of Jurassic ophiolite sequence of the oceanic crust and its Jurassic-Cretaceous sedimentary cover of the Ligurian units, and by the Cretaceous - Oligocene turbidites of the Sub-Ligurian units (Jurassic - Eocene); iii. Tuscan Nappe (Triassic to Miocene) made of evaporites, dolostone, limestones and marls. The Tectonic Wedges complex (Paleozoic-Triassic) made of metamorphic rocks, metasiliciclastics carbonates, and by the Upper Triassic evaporites of the Tuscan Nappe; iv. Crystalline Basement (Pre-Cambrian? - Paleozoic; Pliocene - Quaternary?) formed by the Metamorphic Unit (composed by a Phyllitic complex, a Mica-schist complex, and a Gneiss complex), and the Intrusive complex. Some interpretations of the deep structure of the Larderello geothermal field propose the presence of very large batholites at depth (e.g., Bertini et al., 2006; Romagnoli et al., 2010). Furthermore, other data suggest a still active magmatic emplacement with a partial melt occurring at depth (e.g., Gola et al., 2017 and references therein).

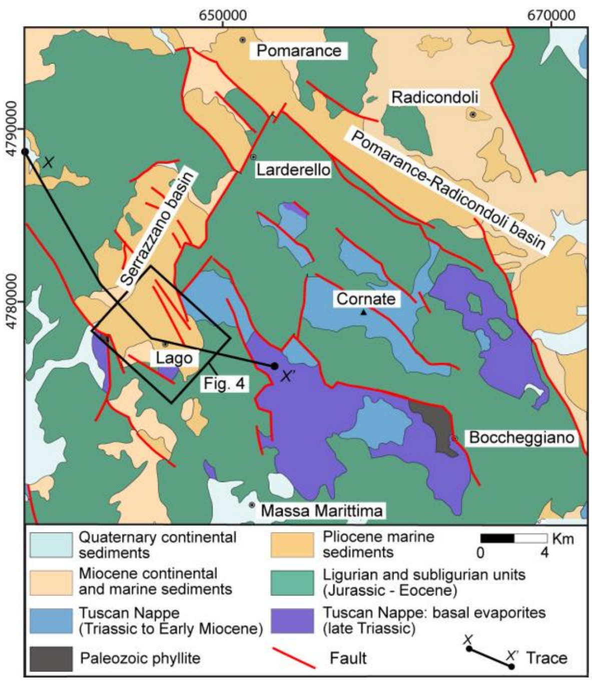

Figure 1: Simplified geological map (in WGS84-UTM32N) of the Larderello geothermal area (modified after de Franco et al., 2019).

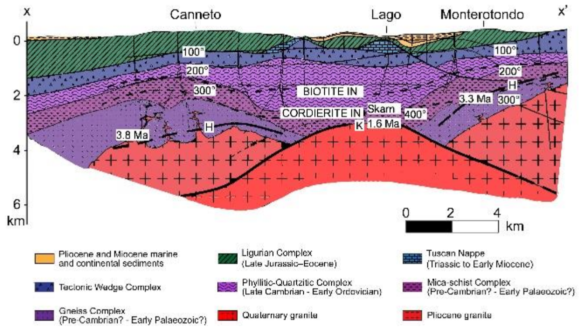

Figure 2: Geological cross-section showing the stratigraphical and tectonic contacts between the various geological complexes (Figure 1 for the location - after de Franco et al., 2019).

3. K-HORIZON

Two important seismic reflectors, named H-horizon and the K-horizon, have been detected in 2D- and recent 3D-seismic surveys of the Larderello geothermal field (Batini et al., 1978; Cameli et al., 1993; Ciuffi and Casini; 2018; Casini et al., 2010 - Figures 3).

The H-horizon is a discontinuous high amplitude reflector and represents a highly productive interval (Bertini et al., 2006). The K-horizon is a high amplitude and locally bright-spot type reflector, it is deeper and barely more continuous than the H-horizon (e.g., Batini et al., 1978; Gianelli et al., 1997; Accaino et al., 2005). In some areas, the K-horizon represents the upper boundary of a zone characterized by seismic reflectors with a lozenge-shape geometry (Cameli et al., 1993).

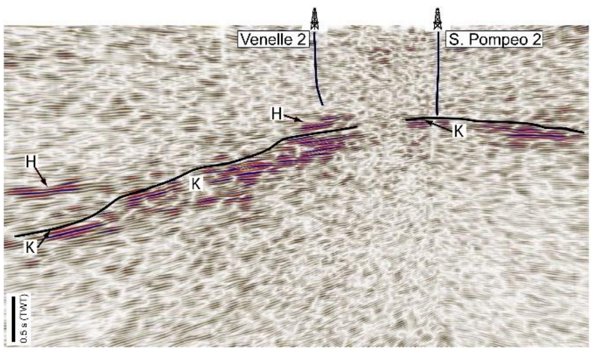

Figure 3: A reflection seismic section from the literature showing the H- and K-horizon (modified after de Franco et al., 2019).

Despite numerous wells have been drilled in the area (Figure 4), the K-horizon has never been reached. The K-horizon origin is still highly debated in the literature and it interpretations derive mainly from seismic line interpretations (Romagnoli et al., 2010; Ciuffi and Casini, 2018; Finetti, 2006). Defining the nature of the K-horizon represents a key to a comprehensive understanding of the Larderello system.

The models proposed in the literature (Table 1) mostly imply the presence of fluids and a correlation with the 450°C ± 50 isotherm (from Liotta and Ranalli, 1999).

The San Pompeo 2 well, drilled in 1982, reached the proximity of the K-horizon but the abrupt increase in temperature and an unexpected blow-out prevented direct measurements at the bottom hole. Temperature greater than 400 °C and pressure greater than 24 MPa were extrapolated at a depth of 2930 m (Batini et al., 1983).

Table 1: Proposed interpretation models of the K-horizon and their related references (after de Franco et al., 2019).

Interpretation model	Source
Mineral phase transition (Quartz α-β)	Marini and Manzella, 2005
Brittle-Ductile Transition with tectonic implication in extensional setting	Cameli et al., 1993 and 1998; Liotta and Ranalli, 1999; Brogi et al., 2003
Rheological variation with tectonic implication in compressive setting	Finetti et al., 2001
Natural hydrofracturing close to lithological or petrophysical changes	Vanorio et al., 2004; De Matteis et al., 2008
Thermometamorphic aureole at the top of Quaternary granites	Bertini et al., 2006
Warm fluids at overpressure conditions	Tinivella et al., 2005

In 2017, the Venelle 2 well was re-drilled and deepened within the framework of the DESCRAMBLE project (Bertani et al., 2018). This well reached a depth of 2909 m without penetrating the K horizon and stopping within well visible seismic reflectors (Ciuffi and Casini, 2018; Bertani et al., 2018). However, the data show that the accentuated seismic reflection at a depth of 2750-2800 m corresponds to a zone of increased thermal gradient (up to 0.3 C°/m and temperature of about 507-517°C at 2900 m) and of decreased pressure fracturing. Pressure decrease is also associated with an increase in both the gas content in drilling fluids and the rate of penetration during drilling activities (Cei and Fiorentini, 2018). The Venelle 2 deepening suggests that the temperature just below the depth of the K-horizon could be as high as 600°C, corresponding to the molten phase of granite, and that the observed increase in the thermal gradient may be the manifestation of a transient thermal state induced by the recent emplacement (<50 ka) of a granitic intrusion (Bertani et al., 2018; Cei and Fiorentini, 2018).

4. DATA AND METHODS

We modelled geological complexes characterized by specific seismic velocities as follow: Neogene deposits, Ligurian complex, Tuscan Nappe and TWC, treated as a single seismic unit as their seismic velocities are similar, and Metamorphic Unit (Figure 2). Faults were not modelled in the present work since their geometry is controversial and poorly defined by the available data.

The 3-D geological-geophysical model has been realized by combining subsurface and superficial data. We used well data, geological information from the literature, subsurface geological maps and a seismic reflection profile (Bertani et al., 2005; Romagnoli et al., 2010). Numerous geothermal wells are present in the study area and data for 69 of them are available from public databases (Figure 4 - Trumpy and Manzella 2017 and references therein).

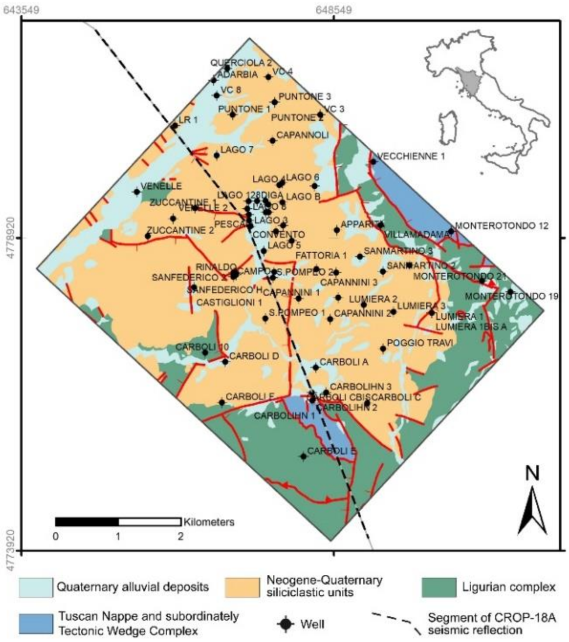

Figure 4: Simplified geological map of the study area. The figure shows the wells used to build the geological model. The segment of the CROP-18A seismic reflection line (Figure 5b) used in the synthetic seismic reflection modelling is reported (modified after de Franco et al., 2019).

The dataset collected were then imported into the Petrel software (Schlumberger) used to generate the 3-D model. In the modelling process, well data were integrated with superficial geological data to better constrain the trend of the modelled surfaces at shallow depths. For the Metamorphic complex and K-horizon surface characterized by few or no well data, we used isobath maps from the literature. The convergent interpolation method with a grid increment of 200 m in x- and y-direction has been used in the modelling process.

The 3D geological-geophysical model was then used to run the synthetic seismic model. The modelled geological surfaces were sampled along a segment of the seismic line CROP-18A. The collected points were subsequently interpolated with a bicubic spline, with 15 m of horizontal spacing.

To create the synthetic seismic section, a velocity model was imposed on the studied section by assigning to each pixel (15x15 m) the P velocities (constant velocity) adopted for the corresponding geological unit in the model calibration (Table 2). Furthermore, we applied a Gaussian velocity perturbation to the velocity model to explore an alternative hypothesis based on the physical rock-model for the K-horizon.

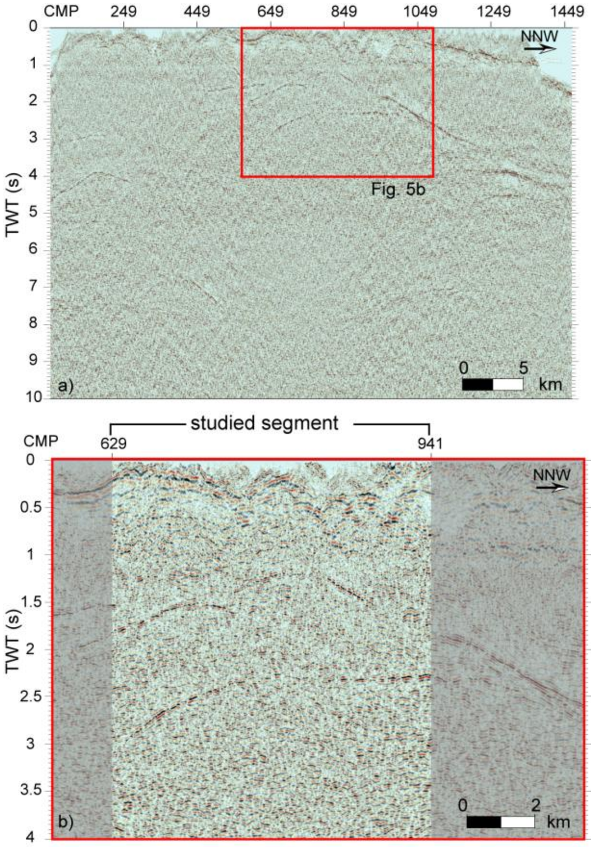

Figure 5: a) CROP18-A stacked section. b) Zoom of the CROP18-A stacked section of Figure 5a. (modified after de Franco et al., 2019).

The synthetic seismic stack sections of the studied segment of the CROP-18A were generated using the exploding reflector seismo-acoustic approach (Loewenthal et al., 1976), developed by the CREWES consortium and partly modified by us. The exploding reflector approach provides a rapid calculation of the zero-offset synthetic stacked sections helping us to calibrate and validate several geological and geophysical interpretative hypotheses of the Larderello geothermal field and, in particular, of the K-horizon. With this approach, the synthetic stacked section is obtained by locating the sources along all reflecting interfaces of the model and the receivers on the common mid points. In the present study the receivers were located at the CMP positions of the line between the CMPs 629 and 941, which were spaced 30 m apart (Figure 5). A time window of up to 4 s of TWT was set (Figure 5).

The exploding reflector approach generates the seismograms for the P-wave velocity model obtained from the section studied. The wavefield is propagated upward through a finite difference algorithm and is then convolved with the input wavelet (Ricker wavelet with 25 Hz of central frequency) to produce the seismogram at the receiver.

To perform the calibration of the reconstructed 2D model along the CROP-18A, we compared the main seismic horizons generated in the synthetic stacked sections processed for different models with the stacked data section along the line.

4 RESULTS AND DISCUSSION

4.1 3D geological-geophysical model

In the modelling process the surfaces modelled were: the topography, the base of the Neogene deposits, the top of the Tuscan Nappe plus TWC, the top of the Metamorphic Unit, and the K-horizon (Figure 6).

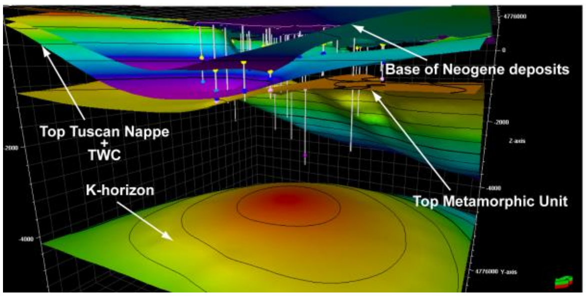

Figure 6: a) Stratigraphic surfaces modelled in Petrel (Schlumberger).

Through these surfaces, we defined the major geological units characterized by specific seismic velocities and, hence, potentially discernible along seismic sections. The modelled interfaces separating the aforementioned geological units were extracted from the 3D geological-geophysical model between the CDP 629 and the CDP 941 of the seismic line CROP-18A and subsequently converted into a time-domain geological-geophysical model.

4.2 Velocity model

The units defined for the velocity model were the Neogene deposits, the Ligurian complex, the Tuscan Nappe plus TWC, the Metamorphic Unit and the geological unit below the K-horizon. A constant P-wave velocity (Vp) was assigned to each unit to obtain the seismic velocity model of the studied segment of the CROP-18A. Table 2 (see the end of the paper) shows the interval velocities applied for the modelled units and the velocity ranges.

For the Neogene Unit and the Ligurian complex, we used the arithmetic average of the interval velocities commonly adopted in the literature (Batini et al., 1978; Brogi et al., 2003). For the Tuscan Nappe plus the TWC, we chose an interval velocity of 5700 m/s. This value was defined after a careful analysis of the data and taking into consideration the wide range of P-wave velocities reported in the literature (e.g., Batini et al., 1978; Brogi et al., 2003). In order to define the velocity value for the Metamorphic Unit, which was set at 5150 m/s, we carefully analyze the data observed in the Vp logs and in laboratory measurements of unfractured rocks from the Mica-schist complex and Gneiss complex in the depth range 1000-3500 m. Seismic reflectivity modelling of the deepest reflective horizons within the metamorphic units based on VSP measurement, logs, and AVO/AVA seismic analysis highlight that reservoir rocks are made up of fractured layers, with a variable thickness from one meter to tens meters, showing a velocity variation of up to 15-30% with respect to the average velocity value of reservoir rocks (Tinivella et al., 2005).

The assignment of a velocity value for the K-horizon and in particular for the unit below the K-horizon is complex and it depends on the geological-geophysical hypotheses of the K-horizon itself. To reduce these uncertainties, we considered two feasible hypotheses for the K-horizon: i) a sharp discontinuity related for example to a lithological change or to an abrupt rheological transition and/or ii) a perturbed layer characterized by an alteration in the physical status of the geological unit. This perturbed layer could be related, for example, to the presence of a thermo-metamorphic aureole, a mineral phase transition, or a highly fractured zone. Results from previous studies suggest a Vp for the unit below the K-horizon ranging between 4300 m/s and 6400 m/s (Rabbel et al., 2017; Vanorio et al., 2004; De Matteis et al., 2008; Accaino et al., 2005; Tinivella et al., 2005). In addition to the uncertainties of each interpretation (about 10%), all these studies agree that the unit below the K-horizon should be assigned a high intrinsic variability of Vp parameter, of up to about 15-40%, with respect to the Vp mean value adopted. In our study, we made test using 4400 m/s and 5900 m/s for the Vp of the unit below the K-horizon corresponding to a contrast of ±15% with respect to the Vp of the upper Metamorphic unit.

4.3 Model calibration and K-horizon characterization by a sharp velocity discontinuity

The geological-geophysical model along the CROP-18A seismic line was calibrated by superimposing the synthetic stacked sections on the seismic data stack for all the reflected events.

In order to evaluate which of the two Vp values proposed in section 4.2 should be used for the unit below the K-horizon (i.e., 4400 m/ and 5900 m/s), we simulated the stacked sections for both velocities. Furthermore, we simulated the stacked sections for two different geological models: Model 1, obtained from the 3D geological-geophysical reconstruction; Model 2 obtained through a calibrated velocity model where the geometry of the K-horizon was modified to produce a better fit of synthetic stacked sections with respect to the section observed. We then compared the seismic features (arrivals and polarities) of the reflection K-horizon with those observed in the data stacked section (Figures 7 and 8). Figures 7 and 8 report the velocity models (on top - a and b) and the synthetic seismic responses (on the bottom - a' and b') for the two Vp values used. Figure 7 shows the results of the original 3D geological-geophysical reconstruction (Model 1), whereas Figure 8 shows the results of the calibrated velocity model (Model 2). The synthetic response (in red variable area) are superimposed onto the stacked data (in grey wiggle and variable area) in order to compare the two zero-offset sections directly.

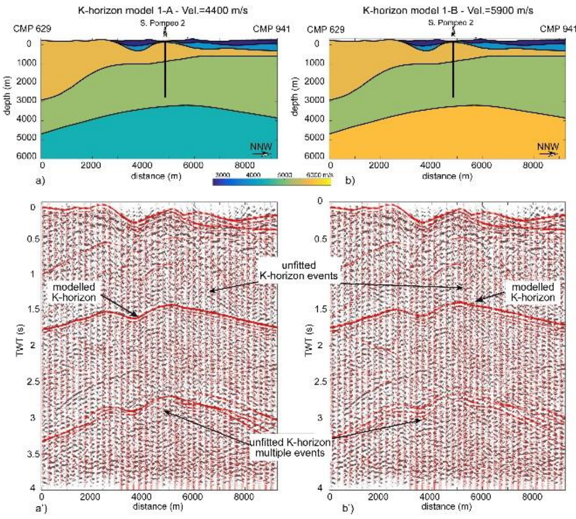

Figure 7: a) and b) Velocity models (Model 1-A and Model 1-B) based on the 3D-geological reconstruction and imposing a velocity value for the unit below the K-horizon of 4400 m/s and 5900 m/s, respectively. a') and b') Modelled stacked sections for Model 1-A and Model 1-B, respectively. (after de Franco et al., 2019).

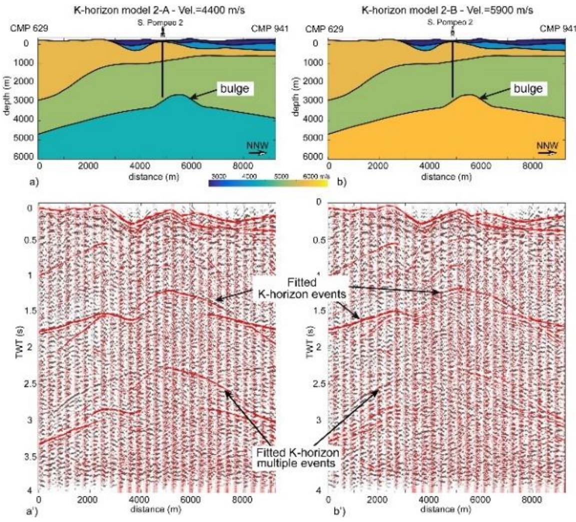

Figure 8: a) and b) Velocity models (Model 2-A and Model 2-B) based on the 3D-geological reconstruction obtained after the calibration with CROP18-A and imposing a velocity value for the unit below the K-horizon of 4400 m/s and 5900 m/s, respectively. a') and b') Modelled stacked sections for Model 1-A and Model 1-B, respectively (after de Franco et al., 2019).

The synthetic seismic responses indicate that Model 2 is comparable with the seismic line drawing of all the main seismic reflection events discernible on the stacked CROP-18A line (Figure 8). For the K-horizon, the best seismic response of Model 2 (Figure 8) was obtained by introducing a bulge like structure located below the S. Pompeo 2 well area not present in the 3D geological-geophysical model (Model 1; Figure 7).

The trace time lags obtained with trace cross-correlations between the data and synthetics signals calculated for the two velocities, in a window of 200 ms TWT including the K-event, have mean values of 5 ms and 18 ms and standard deviations of 40 ms and 73 ms, for 5900 m/s and 4400 m/s, respectively (Figure 8). The 5900 m/s simulation is characterized by the best fit with data and has a mean time lag comparable to the data sampling time of 4 ms. It reproduces the diffractions in the primary reflection between 1.2 s and 2 s TWT and the multiple events (Figure 8). In addition to the reliability of the reconstructed 3D geological-geophysical model, the results obtained by the seismic modelling indicate that: a) the seismic response for TWTs higher than 0.5 s is mainly influenced by the geometry of shallow units; b) due to migration effects, the shape of the modelled K-horizon event in the distance range 2500-7500 m of the unmigrated seismic sections mainly depends on the geometry of the K-horizon in the model distance range of 4400-6700 m. The K-horizon in Model 2 is characterized by a slightly more complex geometry than the reconstructed smoothed K-horizon of Model 1, and introduces a more complex pattern of the K-related events into the time domain with unmigrated diffracted and multiple events also below the K-horizon. This pattern is in line with observations in the data stacked section. Consequently, when interpreting unmigrated K-events in the seismic section, there is a risk of assigning structural and physical meaning to non-existent structures.

4.4 K-horizon alternative hypotheses and modelling: Physically Perturbed Layer

The K-horizon exhibits some very particular reflective seismic features. It shows a lateral variation of reflectivity and it is occasionally characterized by a bright spot signature. Also, instead of single reflection events, it shows a diffuse reflectivity spatially and vertically localized sometimes with a "lozenge" pattern below the top of the diffused reflective events (Cameli et al., 1993). The processing and analyses of several seismic lines in the study area reported in the literature and our results (Section 4.3) highlight that the geological-geophysical models and the related migration velocity models need to be more detailed in order to correctly migrate the reflectivity features observed in seismic section. An alternative hypothesis that we considered is that the K-horizon is associated with a physically perturbed layer, as already claimed by Riedel et al. (2015). This hypothesis is supported by geological evidences on Elba Island, which could be considered as an outcropping analogue of the level of the seismic K-horizon (Zucchi et al., 2017). The results of geological studies carried out on the Elba outcrops suggest that the K-horizon is characterized by a permeability in the range 10^{-9} and 10^{-18} m^2, and by fluid circulation inferred from the fluid inclusions of Elba. We hence considered the K-horizon as a physically perturbed layer (PPL) characterized by a randomized P-wave velocity distribution deriving from the variations of the geological and physical properties.

The high pore pressure in the region of a single fluid-filled pore helps to explain the resulting changes in the effective density and seismic velocities. Increased pressure within a pore tends to force the surrounding rock grains apart, thus tending to increase the pore volume. Effective density is a combination of the densities of the rock and fluid constituents of the porous medium. An increase in porosity results in a decrease in the effective density of the porous medium, as the rock is generally denser than fluid. A decrease in effective density tends to cause an increase in S-wave velocity. The effect of increased pore pressure on P-wave velocity can be seen by considering Wyllie's time-average equation for P-wave velocity in porous, isotropic, fluid-saturated rocks under high pressure (Wyllie et al., 1956). Mavko et al., (2009) interpreted Wyllie's equation as follows: The P-wave travel time through a fluid-saturated rock is equal to the sum of the travel time through the rock matrix and the fluid-filled pore.

In our model, we assume that the detection spatial scale of the velocity variations with seismic is comparable with the ¼ seismic wavelength (several ten of meters).

The pixel values (15x15 m) of the velocity perturbations inside the layer are assumed to be randomized with an asymmetric Gaussian velocity distributions according the velocity variations observed in data logs, laboratory measurements, VSP and AVO-AVA analyses. With an asymmetric distribution, the pixel velocities are set by fixing the highest Vp of the PPL to 5900 m/s whereas its negative variations are defined by the rock physical model described below.

In order to insert a velocity perturbation that is consistent with a rock physical model, we assume that the confining pressure is equal to the lithostatic charge, and that the pore pressure is equal to the hydrostatic charge, and the effective pressure is the difference between them. We assume a temperature of about 400° C, and an effective pressure of about 30 MPa, which is in line with those derived from the measurement in the S. Pompeo 2 well (Batini et al., 1983). A porosity of 3% and a density of 2700 kg/m^3 were used (Zappone and Bruijn, 2012; Orlando, 2005; Zucchi et al., 2017). To calculate the negative velocity variations inside the PPL, we calculated the effective velocities using the scattering theory, considering a prolate (0.02 parameter) penny crack shape that characterizes the fluid inclusions. To simulate the effect of the fluid in the pore and fracture space, we used the values for the velocity and density of brine (1000 m/s and 900 kg/m^3) proposed by Batzle and Wang (1992). Starting from a velocity of 5900 m/s for the unit below the K-horizon, we obtain the minimum velocity values of about 4500 m/s due to the presence of fluid-filled fractured layers, which represents the minimum value for the PPL velocity distribution. Furthermore, this value is about 11% less than the velocity value (5150 m/s) assigned to the overlying metamorphic rocks, causing negative velocity contrasts at the upper boundary of K-horizon.

On the basis of the geological evidence observed on Elba analogue, three models were created: a model with the bulge structure below the San Pompeo 2 well characterized by a perturbed zone, and two models with continuous perturbed layers thick 100 m and 500 m, respectively. We show here only the results of the perturbed layers of 100 m in thickness (Figure 9).

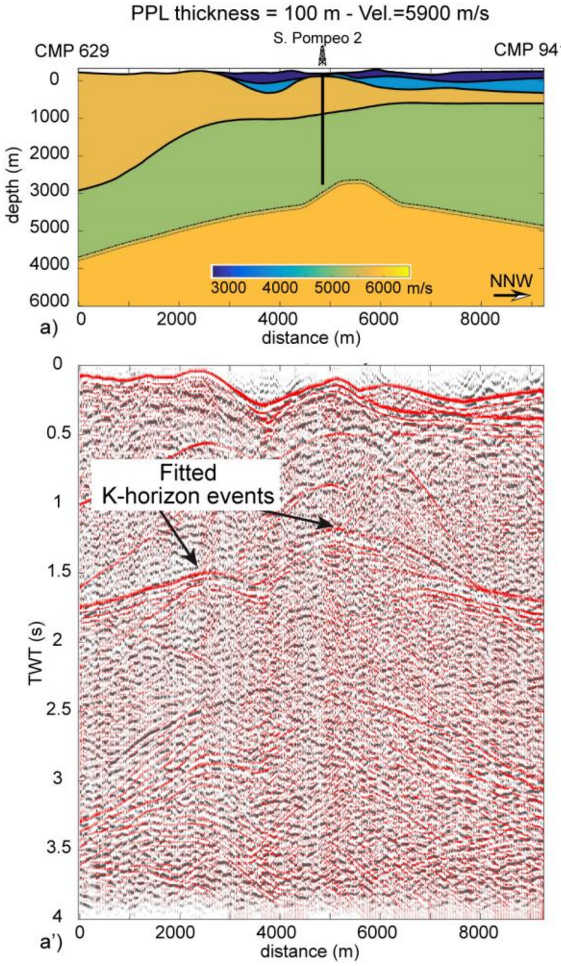

Figure 9: a) Velocity model with a physical perturbed layer of 100 m in thickness; b') Modelled stacked section for the velocity model in Figure 9-a (modified after de Franco et al., 2019).

In the synthetic response with a PPL of 100 m in thickness (Figures 9), the K-horizon reflectivity at the extremities and at the base of the bulge becomes less continuous and reproduces a response that is more in agreement with the original stacked data than the other two synthetic models with a PPL. The main difference between the calibrated velocity model with a sharp discontinuity (Figure 8-b') and that with a PPL of 100 m in thickness is in slight perturbations of K-horizon event times, which are within the best-fit error limits, and in the lateral discontinuity of the signal amplitudes of the K-horizon event in the PPL model. The amplitude lateral variation is the main reason for considering the PPL model as a more suitable physical model than Model 2-B (Figure 8-b'). The PPL may describe the amplitude features of the K-horizon reflection events observed in seismic explorations in the Tuscan geothermal region.

7 CONCLUSIONS

The origin of strong amplitude seismic reflectivity, named K-horizon, below the geothermal reservoirs of Larderello, Tuscany (Italy), has been debated for decades. In our paper, we contribute to the discussion on the origin of the K-horizon by considering two hypotheses: i) a sharp discontinuity and ii) a perturbed layer characterized by an alteration in the physical status of the geological unit.

Our results show that the best fit is obtained by a PPL of 100 m in thickness with a randomized P-wave velocity distribution. The PPL could be representative of a fractured horizon filled by deep fluids possibly at supercritical conditions. The presence of a PPL is in agreement with the various hypotheses proposed in the literature for the K-horizon (Table 1). Furthermore, the PPL hypothesis is supported by the fact that the H-horizon, characterized by fractured rocks with pressurized fluids, has a comparable seismic features.

Others interesting results:

- Deep reflection events are influenced by the articulated shallow morphology of Neogene and Ligurian units. Hence, these effects should be considered in the seismic data processing.
- The seismic modelling with a Vp value of 5900 m/s for the unit below the K-horizon is characterized by the best fit with data. These Vp values are similar to those reported for granites suggesting a granitic intrusion below the K-horizon.
- As different PPL thicknesses show a different seismic pattern of the reflectivity of the K-horizon, the lateral variation of reflectivity of the K-horizon, its bright spot signature, and the diffuse reflectivity could be a consequence of a lateral thickness variation in the PPL.
- Reflectivity depends on the actual structure at the microscale, which cannot be directly reconstructed in detail from the processing of surface seismic data.
- An optimized seismic exploration strategy requires increasing in the resolution of surface seismic, by, as an example, integrating it with VSP data to visualize in detail the diffuse reflectivity zone detected by surface seismic.

Table 2: Interval velocities used in the present work and their ranges from the literature. Interval velocity of the geological unit below the K-horizon represents a major issue for the seismic exploration in the Larderello area and it depends on the geological-geophysical interpretative hypotheses assigned to the K-horizon itself (see text for details); after de Franco et al., 2019.

Layer	V. Int. (m/s)	V. Int. range (m/s)	Source
Neogene deposits	2700	2600-2800	Batini et al., 1978
Ligurian Flysch complex	3850	3000-4700	Batini et al., 1978
Tuscan units and TWC	5700	4000-6500 *3	Batini et al., 1978 and 1995; Brogi et al., 2003
Metamorphic Unit	5150	4400-5500	*1
Unit below the K-horizon	4400/5900	4300-6400	*2

*1 Batini et al., 1978 and 1995; Bertani et al., 2005; Brogi et al., 2003; Rabbel et al., 2017
*2 Batini et al., 1995 and 2002; Vanorio et al., 2004; Tinivella et al., 2005; Aleardi and Mazzotti, 2014; Rabbel et al., 2017
*3 In Brogi et al., 2003, the Tuscan Nappe is divided in two subunits which are the TN 2 (Early Miocene-Rhetic sequence) and the TN 1 (Late Triassic evaporites) with 4000-4500 m/s and 5000-6500 m/s of P-wave interval velocity, respectively.

REFERENCES

Accaino F., Tinivella U., Rossi G., Nicolich, R.: Imaging of CROP-18 deep seismic crustal data. *Boll. Soc. Geol. It.*, (2005), Volume Speciale n. 3, 195-204.

Aleardi M., Mazzotti A.: A feasibility study on the expected seismic AVA signatures of deep fractured geothermal reservoirs in an intrusive basement. *Journ. Geophys. Eng., 11* (6) (2014).

Batini, F., Bertini, G., Bottai, A., Burgassi, P. D., Cappetti, G., Gianelli, G., Puxeddu, M.: San Pompeo 2 deep well: a high temperature and high pressure geothermal system. *In European geothermal update. International seminar*, (1983), 3, 341-353.

Batini F., Burgassi P.D., Cameli G.M., Nicolich R., Squarci P.: Contribution to the study of the deep lithospheric profiles: «deep» reflecting horizons in Larderello-Travale geothermal field. *Mem. Soc. Geol. It.*, (1978), 19, 477-484.

Batzle M. and Wang Z: Seismic properties of pore fluids. *Geophysics*, (1992), 57, 1396–1408.

Barelli, A., Cappetti, G., Stefani, G: Results of deep drilling in the Larderello-Travale/Radicondoli geothermal area, *Proceedings of the Geothermal Congress* (1995), Florence, Italy, 1275–1278.

Bertani, R., Bertini G., Cappetti, G., Fiordelisi, A., and Marocco, B.M.: An update of the Larderello-Travale/Radicondoli deep geothermal system. *Proceedings World Geothermal Congress*, 2005, Antalya, Turkey (2005).

Bertani, R., 2018. DESCRAMBLE Project Conclusive Remarks. *DESCRAMBLE Project, Final Conference*, (2018), Pisa. http://www.descramble-h2020.eu/index.php/events/conferences.

Bertini, G., Casini, M., Gianelli, G., and Pandeli E.: Geological structure of a long-living geothermal system, Larderello, Italy. *Terra Nova*, (2006), 18, 163-169.

Brogi, A., Lazzarotto, A., Liotta, D., Ranalli, G.: Extensional shear zones as imaged by reflection seismic lines: the Larderello geothermal field (Central Italy). *Tectonophysics*, (2003), 363, 127-139.

Cameli, G.M., Dini, I., Liotta D.: Upper crustal structure of the Larderello geothermal field as a feature of post-collisional extensional tectonics (Southern Tuscany, Italy). *Tectonophysics*, (1993), 224, 413-423.

Casini, M., Ciuffi, S., Fiordelisi, A., Mazzotti, A., Stucchi, E.:.Results of a 3D Seismic Survey at Travale geothermal field (Italy). *Geothermics*, (2010), 9, 4–12.

Cei M. and Fiorentini A.: Resource characterization post drilling. *DESCRAMBLE Project, Final Conference*, (2018), Pisa.

Ciuffi, S. and Casini, M., 2018. VSP and target definition. *DESCRAMBLE Project, Final Conference*, (2018), Pisa.

CREWES - Consortium for Research in Elastic Wave Exploration Seismology. CREWES MATLAB Toolbox. University of Calgary. https://www.crewes.org/ResearchLinks/FreeSoftware/

de Franco, R., Petracchini, L., Scrocca, D., Caielli, G., Montegrossi, G., Santilano, A., Manzella, A. Synthetic seismic reflection modelling in a supercritical geothermal system: an image of the K-horizon in the Larderello field (Italy) (2019). Accepted 4 November 2018 on *Geofluids* (Hindawi).

De Matteis, R., Vanorio, T., Zollo, A., Ciuffi, S., Fiordelisi, A., Spinelli, E.: Three-dimensional tomography and rock properties of the Larderello-Travale geothermal area, Italy. *Physics of the Earth and Planetary Interiors*, (2008), 168, 37–48.

Finetti, I. R.: Basic regional crustal setting and superimposed local pluton-intrusion-related tectonics in the Larderello-M. Amiata geothermal province, from integrated CROP seismic data. *Bollettino della Società geologica italiana*, (2006), 125(1), 117-146.

Finetti I.R., Boccaletti, M., Bonini, M., Del Bena, A., Geletti, R., Pipan, M., Sani, F.: Crustal section based on CROP seismic data across the North Tyrrhenian–Northern Apennines–Adriatic Sea. *Tectonophysics*, (2001), 343, 135–163.

Gianelli, G., Manzella, A., Puxeddu, M.: Crustal models of the geothermal areas of Southern Tuscany. *Tectonophysics* 281, (1997), 221 – 239.

Gola, G., Bertini, G., Bonini, M., Botteghi, S., Brogi, A., De Franco, R., Dini, A., Donato, A., Gianelli, G., Liotta, D., Manzella, A., Montanari, D., Montegrossi, G., Petracchini, L., Ruggieri, G., Santilano, A., Scrocca, D. and Trumpy, E.: Data integration and conceptual modelling of the Larderello geothermal area, Italy. *Energy Procedia*, 125, (2017), 300-309.

Liotta, D. and Ranalli, G.: Correlation between seismic reflectivity and rheology in extended lithosphere: southern Tuscany, Inner Northern Apennines, Italy. *Tectonophysics*, (1999), 315, 109–122.

Loewenthal, D., Lu, L., Roberson R., Sherwood J.: The wave equation applied to migration. *Geophys. Prosp.*, (1976), 24, 380-399.

Mavko, G., Mukerji, T., Dvorkin, J.: The rock physics handbook: Tools for seismic analysis of porous media. *Cambridge university press*, (2009).

Marini, L., and Manzella, A.: Possible seismic signature of the α-β quartz transition in the lithosphere of Southern Tuscany (Italy). *Journal of Volcanology and Geothermal Research*, (2005), 148, 81- 97.

Minissale, A.: The Larderello geothermal field: a review. *Earth-Science Reviews*, (1991), 31(2), 133-151.

Orlando, L.: Interpretation of Tuscan gravity data. *Bollettino Società Geologica Italiana*, (2005), 179-186.

Rabbel, W., Jusri, T., Köhn, D., Motra, H. B., Niederau, J, Schreiter, L., Thorwart, M., Wuttke, F. (the DESCRAMBLE Working Group): Seismic Velocity Uncertainties and their Effect on Geothermal Predictions: A Case Study. *Energy Procedia*, (2017), 125, 283–290.

Riedel, M., Dutsch, C., Alexandrakis, C., Dini, I., Ciuffi, S., and Buske, S.: Seismic depth imaging of a geothermal system in Southern Tuscany. *Geophysical Prospecting*, (2015), 63(4), 957-974.

Romagnoli. P., Arias. A., Barelli. A., Cei. M. and Casini, M.: An updated numerical model of the Larderello–Travale geothermal system, Italy. *Geothermics*, (2010), 39, 292–313.

Schmelzbach, C., Greenhalgh, S., Reiser, F., Girard, J. F., Bretaudeau, F., Capar, L., and Bitri, A.: Advanced seismic processing/imaging techniques and their potential for geothermal exploration. *Interpretation*, (2016), 4(4), SR1-SR18.

Tinivella U., Accaino F., Rossi G., Nicolich R.: Petrophysical analysis of CROP-18 crustal seismic data. *Bollettino Società Geologica Italiana*. (2005), Vol spec., 205-211.

Trumpy, E., and Manzella, A.: Geothopica and the interactive analysis and visualization of the updated Italian National Geothermal Database. *International Journal of Applied Earth Observation and Geoinformation*, (2017), 54, 28-37.

Scrocca D., Doglioni C., Innocenti F., Manetti P., Mazzotti A., Bertelli L., Burbi L., Doffizi S. (Eds): CROP Atlas: seismic reflection profiles of the Italian crust. *Memorie Descrittive della Carta Geologica d'Italia*, (2003),62, 1-194.

Vanorio, T., De Matteis, R., Zollo, A., Batini, F., Fiordelisi, A., Ciulli, B.: The deep structure of the Larderello-Travale geothermal field from 3D microearthquake traveltime tomography. *Geophys. Res. Lett.*, (2004), 32.

Zappone, A. S., and Bruijn, R. H.: The Swiss atlas of physical properties of rocks (SAPHYR). Rapport Annuel. (2012).

Zucchi, M., Brogi, A., Liotta, D., Rimondi, V., Ruggieri, G., Montegrossi, G., Caggianelli, A., Dini, A.: Permeability and hydraulic conductivity of faulted micaschist in the eastern Elba Island exhumed geothermal system (Tyrrhenian sea, Italy): insights from Cala Stagnone. *Geothermics*, (2017).,70, 125-145.

Wyllie, M.R.J., Gregory, A.R., and Gardner, L.W., 1956. Elastic wave velocities in heterogeneous and porous media. *Geophysics*, (1956), 21, 41-70.

Acknowledgements

This work was supported by the EU FP7-funded Integrated Methods for Advanced Geothermal Exploration (IMAGE) Project under grant agreement [608553]